

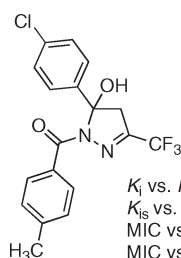
# Discovery and Development of the Covalent Hydrates of Trifluoromethylated Pyrazoles as Riboflavin Synthase Inhibitors with Antibiotic Activity Against *Mycobacterium tuberculosis*

Yujie Zhao,<sup>†</sup> Adelbert Bacher,<sup>‡</sup> Boris Illarionov,<sup>§</sup> Markus Fischer,<sup>§</sup> Gunda Georg,<sup>¶</sup> Qi-Zhuang Ye,<sup>¶</sup> Phillip E. Fanwick,<sup>#</sup> Scott G. Franzblau,<sup>⊥</sup> Baojie Wan,<sup>⊥</sup> and Mark Cushman<sup>\*,†</sup>

<sup>†</sup>Department of Medicinal Chemistry and Molecular Pharmacology, School of Pharmacy and Pharmaceutical Sciences, and The Purdue Cancer Center, Purdue University, West Lafayette, Indiana 47907, <sup>‡</sup>Ikosatec GmbH, Königsbergerstrasse 74, 85748 Garching, Germany, <sup>§</sup>Institute of Biochemistry and Food Chemistry, Food Chemistry Division, University of Hamburg, D-20146 Hamburg, Germany, <sup>¶</sup>Department of Medicinal Chemistry, University of Kansas, Lawrence, Kansas 66047, <sup>#</sup>Department of Chemistry, Purdue University, West Lafayette, Indiana 47907, and <sup>⊥</sup>Institute for Tuberculosis Research, College of Pharmacy, University of Illinois at Chicago, Chicago, Illinois 60612

cushman@pharmacy.purdue.edu

Received April 13, 2009



$K_i$  vs. *M. tuberculosis* riboflavin synthase  $23 \pm 14 \mu\text{M}$   
 $K_{is}$  vs. *M. tuberculosis* riboflavin synthase  $10 \pm 2 \mu\text{M}$   
 MIC vs. *M. tuberculosis* replicating phenotype  $50 \pm 3.6 \mu\text{M}$   
 MIC vs. *M. tuberculosis* non-replicating phenotype  $56 \pm 3.5 \mu\text{M}$

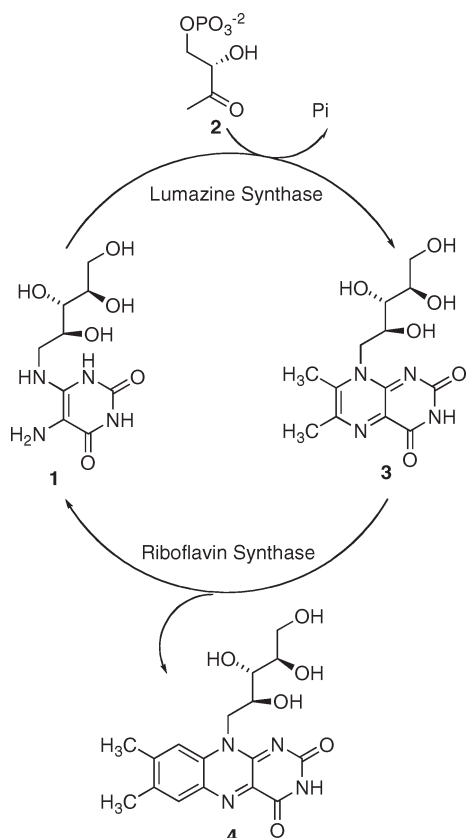
A high-throughput screening (HTS) hit compound displayed moderate inhibition of *Mycobacterium tuberculosis* and *Escherichia coli* riboflavin synthases. The structure of the hit compound provided by the commercial vendor was reassigned as [3-(4-chlorophenyl)-5-hydroxy-5-(trifluoromethyl)-4,5-dihydro-1H-pyrazol-1-yl](*o*-tolyl)methanone (**18**). The hit compound had a  $k_{is}$  of  $8.7 \mu\text{M}$  vs. *M. tuberculosis* riboflavin synthase and moderate antibiotic activity against both *M. tuberculosis* replicating phenotype and nonreplicating persistent phenotype. Molecular modeling studies suggest that two inhibitor molecules bind in the active site of the enzyme, and that the binding is stabilized by stacking between the benzene rings of two adjacent ligands. The most potent antibiotic in the series proved to be [5-(4-chlorophenyl)-5-hydroxy-3-(trifluoromethyl)-4,5-dihydro-1H-pyrazol-1-yl](*m*-tolyl)methanone (**16**), which displayed a minimum inhibitory concentration (MIC) of  $36.6 \mu\text{M}$  vs. *M. tuberculosis* replicating phenotype and  $48.9 \mu\text{M}$  vs. *M. tuberculosis* nonreplicating phenotype. The HTS hit compound and its analogues provide the first examples of riboflavin synthase inhibitors with antibiotic activity.

## Introduction

Riboflavin (**4**), also known as vitamin B<sub>2</sub>, is the central component of the cofactors FAD and FMN, and is therefore required for a wide variety of cellular processes. It plays a key role in energy production, and is required for the metabolism of fats, carbohydrates, and proteins. Whereas animals acquire riboflavin completely from dietary sources, plants and pathogenic microorganisms rely on biosynthesis. Since the riboflavin biosynthetic pathway is absent in the human host, inhibition of the pathway should be selectively toxic to the pathogen and not to the host. Riboflavin synthase and lumazine synthase, the last

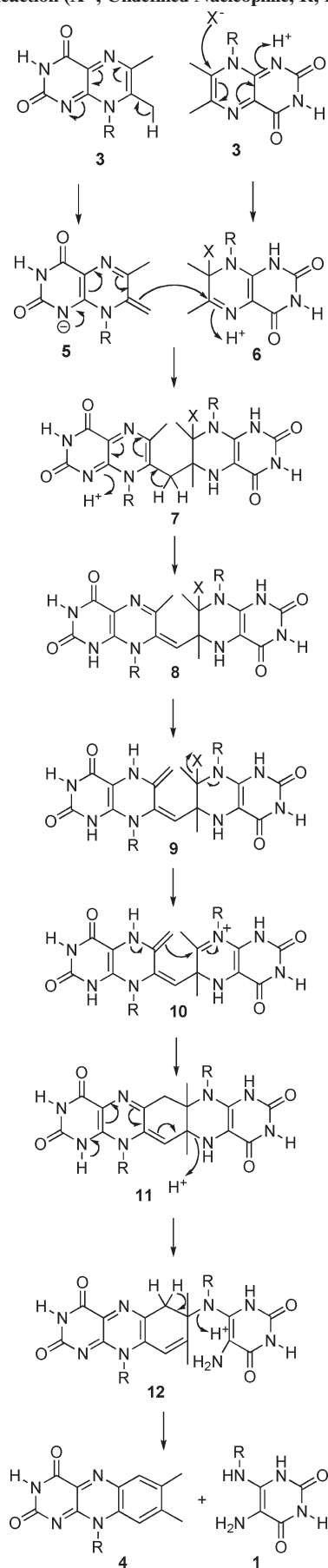
two enzymes in the riboflavin biosynthetic pathway (Scheme 1), are therefore targets for the design of potential antibiotics.<sup>1–5</sup>

- (1) Bacher, A.; Eberhardt, S.; Fischer, M.; Kis, K.; Richter, G. *Annu. Rev. Nutr.* **2000**, *20*, 153–167.
- (2) Kis, K.; Volk, R.; Bacher, A. *Biochemistry* **1995**, *34*, 2883–2892.
- (3) Gerhardt, S.; Schott, A.-K.; Kairies, N.; Cushman, M.; Illarionov, B.; Eisenreich, W.; Bacher, A.; Huber, R.; Steinbacher, S.; Fischer, M. *Structure* **2002**, *10*, 1371–1381. Figure 1 has been reproduced from this reference with permission from Elsevier.
- (4) Illarionov, B.; Eisenreich, W.; Bacher, A. *Proc. Natl. Acad. Sci. U.S.A.* **2001**, *98*, 7224–7229.
- (5) Illarionov, B.; Kemter, K.; Eberhardt, S.; Richter, G.; Cushman, M.; Bacher, A. *J. Biol. Chem.* **2001**, *276*, 11524–11530.

**SCHEME 1. The Last Two Steps in the Riboflavin Biosynthetic Pathway**

The final step in the biosynthesis of riboflavin is catalyzed by riboflavin synthase. A hypothetical mechanism for the formation of riboflavin is outlined in Scheme 2. The early steps in this proposal involve the addition of a nucleophile to the lumazine **3** that will function as the donor of the four-carbon unit to form **6**, and the deprotonation of the C-7 methyl group of the lumazine **3** that will function as the acceptor of the four-carbon unit to form the anion **5**.<sup>6–8</sup> Although the identity of the nucleophile has not been rigorously established, likely candidates include water or one of the ribityl hydroxyl groups.<sup>9,10</sup> Nucleophilic addition of the anion **5** to the imine **6** affords intermediate **7**, which tautomerizes to yield intermediate **8**. Elimination of the anion  $X^-$  from **9** results in the iminium ion **10**, which is attacked intramolecularly by the enamine to produce the pentacyclic intermediate **11**. The pentacyclic compound **11** has been isolated and shown to be a kinetically competent intermediate, and its structure has been established by multinuclear NMR spectroscopy.<sup>4</sup> Two sequential elimination reactions then produce the final products **1** and **4**.

Riboflavin synthase is characterized by an internal sequence repeat within each homotrimer subunit, which suggests that each riboflavin monomer contains two topologically similar domains,

**SCHEME 2. Hypothetical Mechanism of the Riboflavin Synthase-Catalyzed Reaction ( $X^-$ , Undefined Nucleophile; R, Ribityl Chain)**

(6) Beach, R. L.; Plaut, G. W. E. *J. Am. Chem. Soc.* **1970**, *92*, 2913–2916.

(7) Beach, R. L.; Plaut, G. W. E. *J. Am. Chem. Soc.* **1971**, *93*, 3937–3943.

(8) Paterson, T.; Wood, H. S. C. *J. Chem. Soc., Perkin Trans. 1* **1972**, 1051–1056.

(9) Cushman, M.; Patrick, D. A.; Bacher, A.; Scheuring, J. *J. Org. Chem.* **1991**, *56*, 4603–4608.

(10) Bown, D. H.; Keller, P. J.; Floss, H. G.; Sedlmaier, H.; Bacher, A. *J. Org. Chem.* **1986**, *51*, 2461–2467.

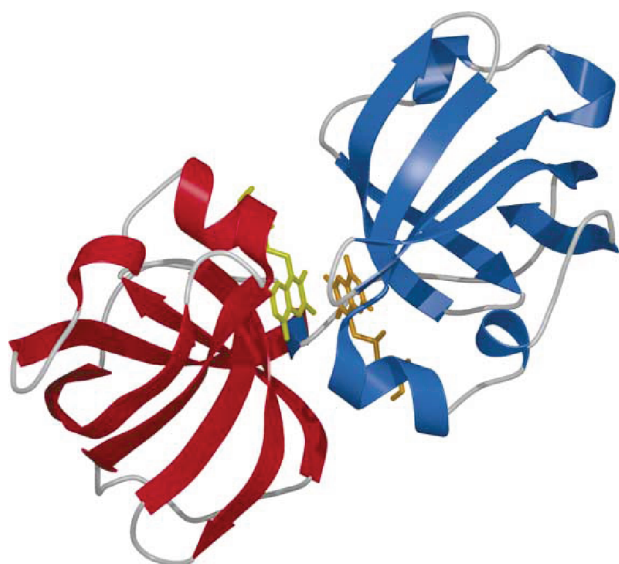
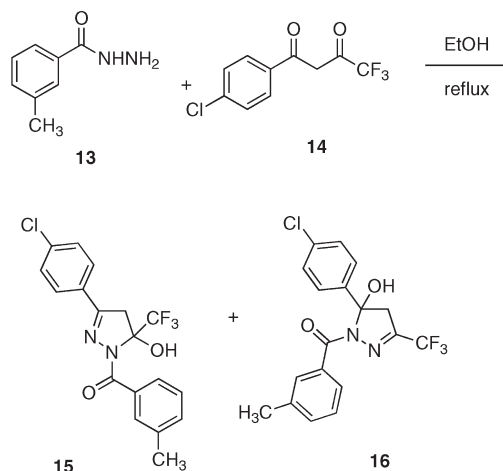


**FIGURE 1.** Hypothetical structure of the active site dimer of *S. pombe* riboflavin synthase with bound substrate **3**.<sup>3</sup>

each of which can accommodate one substrate molecule.<sup>9,11–14</sup> The active site has been proposed to be located at the interface of adjacent subunits (Figure 1).<sup>3</sup> More specifically, two substrate lumazine molecules are assumed to be sandwiched in a tight intermolecular interface between the N-terminal domain from one subunit and the C-terminal domain from an adjacent subunit. Figure 1 displays the two barrel domains of adjacent subunits viewed along a pseudo-2-fold symmetry axis and two molecules of bound substrate **3** in the active site, where two molecules of **3** are ideally positioned for the dismutation reaction.<sup>3</sup>

We have previously reported the structure-based design and synthesis of lumazine synthase and riboflavin synthase inhibitors that are useful mechanism probes.<sup>9,12,13,15–30</sup>

### SCHEME 3. Syntheses of Compounds **15** and **16**



However, those compounds are very polar substrate, intermediate, and product analogues that cannot be expected to be able to penetrate cells membranes and exert antibiotic activity. High-throughput screening platforms were therefore developed to provide alternative methods to obtain inhibitors with drug-like properties.<sup>31,32</sup> The method involving riboflavin synthase measures the inhibition of riboflavin formation in the presence of substrate **3**. High-throughput screening of a commercial library of about 100 000 compounds using this assay resulted in 127 hit compounds having IC<sub>50</sub> values of 16.7 µg/mL or less, and the tentative identification of [3-(4-chlorophenyl)-5-hydroxy-5-(trifluoromethyl)-4,5-dihydro-1H-pyrazol-1-yl](*m*-tolyl)methanone (**15**), based on the vendor's structure, as one of the most potent riboflavin synthase inhibitors of the series. The present paper describes the assignment of the correct structure **18** to the hit compound that had been identified as **15** by the vendor, as well as the confirmation of the riboflavin synthase inhibitory activity of **15**, **18**, and related trifluoromethylated, covalently hydrated pyrazoles. This series of compounds provides the first examples of riboflavin synthase inhibitors with antibiotic activity.

### Results and Discussion

In an attempt to confirm the vendor's structure **15** of the hit compound, samples were obtained both commercially (Chem-Div, Inc., CD 3852-0429) and also by synthesis from *m*-toluidine hydrazide (**13**) and 1-(4-chlorophenyl)-4,4,4-trifluoro-1,3-butanedione (**14**) in refluxing ethanol containing a catalytic amount of hydrochloric acid (Scheme 3).<sup>33</sup> Compounds **15** [mp 94–95 °C, negative ion ESIHRMS *m/z* calcd for C<sub>18</sub>H<sub>13</sub>ClF<sub>3</sub>N<sub>2</sub>O<sub>2</sub> (M – H)<sup>+</sup> 381.0618, found 381.0624] and **16** [mp 172–173 °C, ESIHRMS *m/z* calcd for C<sub>18</sub>H<sub>14</sub>ClF<sub>3</sub>N<sub>2</sub>O<sub>2</sub>Na (MNa)<sup>+</sup> 405.0594, found 405.0601] were obtained by flash column chromatography of our synthetic material. The mass spectral data of both compounds are consistent with a molecular weight of 382. The ratio of the products **15** and **16** was approximately 10:1, respectively.

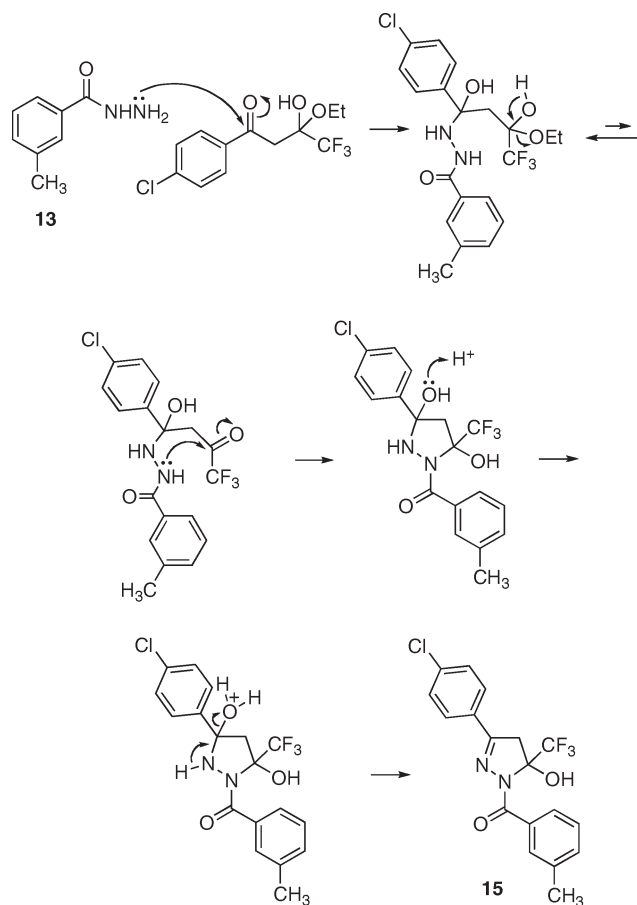
(31) Craig, J. C.; Naik, A. R. *J. Am. Chem. Soc.* **1962**, *84*, 3410.

(32) Kaiser, J.; Illarionov, B.; Rohdich, F.; Eisenreich, W.; Saller, S.; Van den Brulle, J.; Cushman, M.; Bacher, A.; Fischer, M. *Anal. Biochem.* **2007**, *365*, 52–61.

(33) Umarov, B. B.; Gaibullaev, K. S.; Parpiev, N. A. *O'z.b. Resp. Fanlar Akad. Ma'ruzalari* **2000**, *9*, 42–45.

- (11) Otto, M.; Bacher, A. *Eur. J. Biochem.* **1981**, *115*, 511–517.
- (12) Cushman, M.; Patel, H. H.; Scheuring, J.; Bacher, A. *J. Org. Chem.* **1992**, *57*, 5630–5643.
- (13) Cushman, M.; Mavandadi, F.; Kugelbrey, K.; Bacher, A. *Bioorg. Med. Chem.* **1998**, *6*, 409–415.
- (14) Harvey, R. A.; Plaut, G. W. E. *J. Biol. Chem.* **1966**, *241*, 2120–2136.
- (15) Cushman, M.; Patel, H. H.; Scheuring, J.; Bacher, A. *J. Org. Chem.* **1993**, *58*, 4033–4042.
- (16) Scheuring, J.; Lee, J.; Cushman, M.; Pater, H.; Patrick, D. A.; Bacher, A. *Biochemistry* **1994**, *33*, 7634–7640.
- (17) Scheuring, J.; Cushman, M.; Bacher, A. *J. Org. Chem.* **1995**, *60*, 243–245.
- (18) Cushman, M.; Mavandadi, F.; Kugelbrey, K.; Bacher, A. *J. Org. Chem.* **1997**, *62*, 8944–8947.
- (19) Cushman, M.; Mavandadi, F.; Yang, D.; Kugelbrey, K.; Kis, K.; Bacher, A. *J. Org. Chem.* **1999**, *64*, 4635–4642.
- (20) Kendall, P. M.; Johnson, J. V.; Cook, C. E. *J. Org. Chem.* **1979**, *44*, 1421–1424.
- (21) Cushman, M.; Mihalic, J. T.; Kis, K.; Bacher, A. *J. Org. Chem.* **1999**, *64*, 3838–3845.
- (22) Cushman, M.; Yang, D.; Kis, K.; Bacher, A. *J. Org. Chem.* **2001**, *66*, 8320–8327.
- (23) Cushman, M.; Yang, D.; Mihalic, J. T.; Chen, J.; Gerhardt, S.; Huber, R.; Fischer, M.; Kis, K.; Bacher, A. *J. Org. Chem.* **2002**, *67*, 6871–6877.
- (24) Cushman, M.; Yang, D.; Gerhardt, S.; Huber, R.; Fischer, M.; Kis, K.; Bacher, A. *J. Org. Chem.* **2002**, *67*, 5807–5816.
- (25) Cushman, M.; Sambaiah, T.; Jin, G.; Illarionov, B.; Fischer, M.; Bacher, A. *J. Org. Chem.* **2004**, *69*, 601–612.
- (26) Chen, J.; Sambaiah, T.; Illarionov, B.; Fischer, M.; Bacher, A.; Cushman, M. *J. Org. Chem.* **2004**, *69*, 6996–7003.
- (27) Zhang, Y. L.; Jin, G. Y.; Illarionov, B.; Bacher, A.; Fischer, M.; Cushman, M. *J. Org. Chem.* **2007**, *72*, 7176–7184.
- (28) Cushman, M.; Jin, G.; Illarionov, B.; Fischer, M.; Ladenstein, R.; Bacher, A. *J. Org. Chem.* **2005**, *70*, 8162–8170.
- (29) Talukdar, A.; Illarionov, B.; Bacher, A.; Fischer, M.; Cushman, M. *J. Org. Chem.* **2007**, *72*, 7167–7175.
- (30) Zhang, Y. L.; Illarionov, B.; Morgunova, E.; Jin, G. Y.; Bacher, A.; Fischer, M.; Ladenstein, R.; Cushman, M. *J. Org. Chem.* **2008**, *73*, 2715–2724.

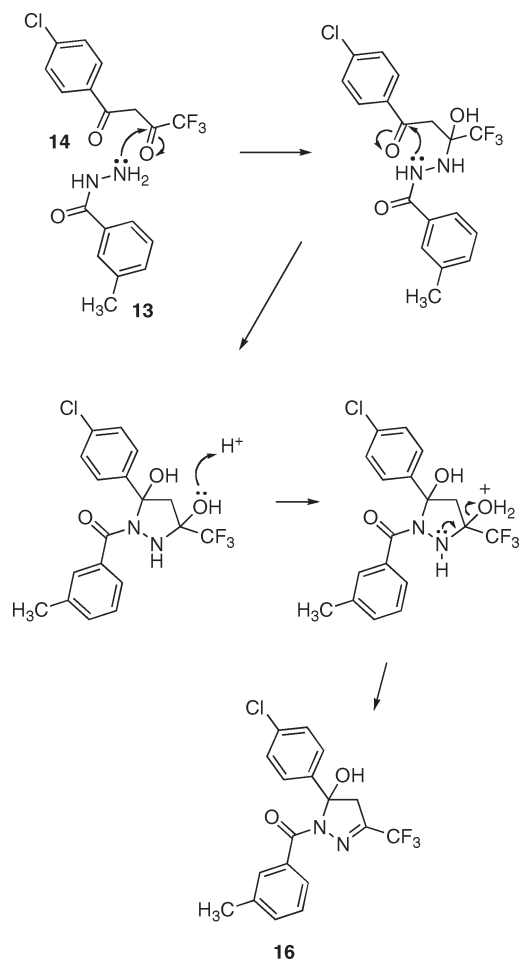
SCHEME 4. Mechanism Proposed for Formation of Compound 15



Mechanisms for the formation of the major product **15** and the minor product **16** are proposed in Schemes 4 and 5. The ketone of **14** bearing the trifluoromethyl group is expected to exist mainly as the hemiketal derived from addition of ethanol, the solvent.<sup>34</sup> Consistent with this expectation was the appearance of a major trifluoromethyl signal  $-6.71$  ppm upfield from  $\text{CF}_3\text{COOH}$  (external standard) and a minor signal  $-1.15$  ppm upfield from  $\text{CF}_3\text{COOH}$  in a  $^{19}\text{F}$  NMR spectrum recorded after **14** was dissolved in dilute ethanolic HCl. The trifluoromethylated hemiketal could explain the preferred regiochemistry of addition of the hydrazine amino group to the carbonyl attached to the *p*-chlorophenyl ring (Scheme 4). On the other hand, the trifluoromethylated carbonyl group of the  $\beta$ -diketone **14**, which is present in the reaction mixture as a minor component, is expected to be more reactive due to the attached highly electronegative trifluoromethyl substituent. Nucleophilic attack of the terminal amino group of the hydrazine **13** on the trifluoromethylated carbonyl of **14** would eventually lead to the minor product **16** (Scheme 5). In both cases, the covalently hydrated pyrazoles are stabilized by the electron-attracting amide moiety and trifluoromethyl substituent. Both **15** and **16** are stable carbinolamides.

Thin layer chromatography indicated that the commercial compound (Chemdiv Co., **CD 3852-0429**) had the same  $R_f$

SCHEME 5. Mechanism Proposed for Formation of Compound 16



values as compound **16** employing different mobile systems. However, their melting points were significantly different: **CD 3852-0429**, mp  $76-78^\circ\text{C}$ ; compound **16**, mp  $172-173^\circ\text{C}$ . Moreover, the  $^1\text{H}$  and  $^{13}\text{C}$  NMR spectral data from the commercial sample (Chemdiv Co., **CD 3852-0429**), which purportedly had structure **15**, did not match with either one of the compounds. The  $^1\text{H}$  NMR spectra of compounds **15** and **16** indicated that they both contain a methylene group in a 4,5-dihydropyrazole ring. The structure assigned to synthetic **15** was confirmed by X-ray crystallography (Figure S4, Supporting Information). At this point, it became clear that **CD 3852-0429** has a different structure than advertised.

To assign the structures of compounds **15** and **16**,  $^{19}\text{F}$  NMR spectra of the synthesized compounds and the commercial compound (Chemdiv Co., **CD 3852-0429**) were analyzed. The trifluoromethyl groups of **CD 3852-0429** and compound **15** both appeared in their  $^{19}\text{F}$  NMR spectra at  $-3.11$  to  $-3.56$  ppm upfield from  $\text{CF}_3\text{CO}_2\text{H}$ , supporting their attachment to  $\text{sp}^3$ -hybridized carbon atoms. Meanwhile, the trifluoromethyl group of compound **16** appeared at  $10.33$  ppm downfield from  $\text{CF}_3\text{CO}_2\text{H}$ , indicating its attachment to an  $\text{sp}^2$ -hybridized carbon atom.<sup>35,36</sup>

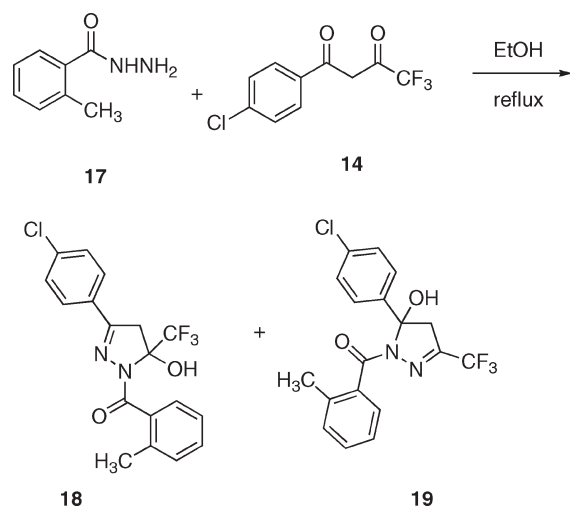
(34) Fustero, S.; Román, R.; Sanz-Cervera, J. F.; Simón-Fuentes, A.; Cuñat, A. C.; Villanova, S.; Murguía, M. *J. Org. Chem.* **2008**, *73*, 3523–3529.

(35) Cushman, M.; Wong, W. C.; Bacher, A. *J. Chem. Soc., Perkin Trans. I* **1986**, 1043–1050.

(36) Cushman, M.; Wong, W. C.; Bacher, A. *J. Chem. Soc., Perkin Trans. I* **1986**, 1051–1053.



## SCHEME 6. Synthesis of Compounds 18 and 19



The synthetic and commercial materials were studied in more detail to explain the observed differences. The commercial sample **CD 3852-0429** had the same molecular weight, similar methylene  $^1\text{H}$  NMR chemical shifts, and similar  $^{19}\text{F}$  NMR chemical shifts as compound **15**. However, the 2D HMBC NMR spectrum of **CD 3852-0429** indicated that the methyl group was coupled to only one adjacent proton, whereas that of **15** provided evidence for two adjacent protons. To elucidate the structure of the commercial sample, a series of isomeric compounds were synthesized and characterized (Schemes 6 and 7). This led to the assignment of the structure of the commercial sample from Chemdiv as [3-(4-chlorophenyl)-5-hydroxy-5-(trifluoromethyl)-4,5-dihydro-1H-pyrazol-1-yl](o-tolyl)methanone (**18**) since the melting point, IR,  $^1\text{H}$  NMR,  $^{13}\text{C}$  NMR, and  $^{19}\text{F}$  NMR of our synthetic compound **18** and the commercial compound were identical. Furthermore, a mixed mp  $79\text{--}81\text{ }^\circ\text{C}$  of **18** and the commercial sample **CD 3852-0429** was not depressed, whereas the mixed mp  $79\text{--}95\text{ }^\circ\text{C}$  of **15** and the commercial sample **CD 3852-0429** was depressed. These results emphasize the necessity to confirm the structures of hit compounds obtained from commercial libraries.

Enzyme kinetics revealed that all six compounds in this series inhibit *M. tuberculosis* riboflavin synthase and *E. coli* riboflavin synthase (Table 1) with  $K_i$  and  $K_{is}$  values in the micromolar range. Compound **19** was the most potent inhibitor of *M. tuberculosis* riboflavin synthase with a  $K_i$  of  $6.7 \pm 1.6\text{ }\mu\text{M}$ , while compound **18** was the most potent inhibitor of *E. coli* riboflavin synthase, with a  $K_i$  of  $31 \pm 10\text{ }\mu\text{M}$  in Tris buffer, pH 7.0.

Molecular modeling was performed in order to investigate the binding of this series of compounds to the enzyme. The crystal structure of *E. coli* riboflavin synthase, a homotrimer that consists of an asymmetric assembly of monomers (molecules A, B, and C), has been published along with a proposed active site between the C-terminal barrel of molecule A and the N-terminal barrel of molecule C (PDB code 1i8d).<sup>37</sup> A crystal structure has also been determined of monomeric *S. pombe* riboflavin synthase with bound substrate analogue 6-carboxyethyl-7-oxo-8-ribityllumazine (PDB code 1kzl).<sup>3</sup>

(37) Liao, D.-I.; Wawrzak, Z.; Calabrese, J. C.; Viitanen, P. V.; Jordan, D. B. *Structure* **2001**, 9, 399–408.

## SCHEME 7. Synthesis of Compounds 21 and 22

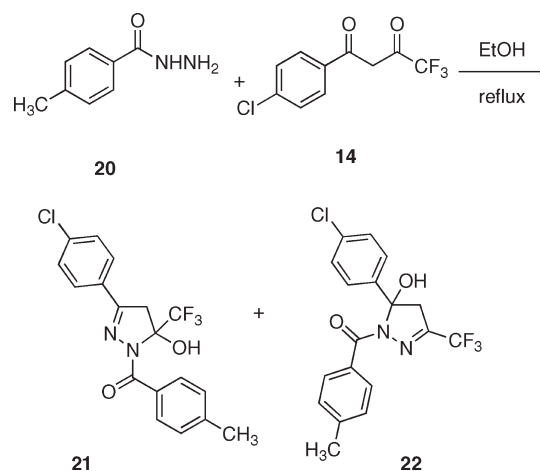


TABLE 1. Inhibition Constants vs. Riboflavin Synthases from *M. tuberculosis* and *E. coli*

| compd     | parameter                    | <i>M. tuberculosis</i><br>riboflavin synthase | <i>E. coli</i> riboflavin<br>synthase |
|-----------|------------------------------|---|---------------------------------------|
| <b>15</b> | $K_i^a$ ( $\mu\text{M}$ )    | $14 \pm 3$                                    | $106 \pm 31$                          |
|           | $K_{is}^b$ ( $\mu\text{M}$ ) | $38 \pm 11$                                   | $91 \pm 17$                           |
|           | mechanism                    | partial                                       | partial                               |
| <b>16</b> | $K_i$ ( $\mu\text{M}$ )      |   | $50 \pm 14$                           |
|           | $K_{is}$ ( $\mu\text{M}$ )   | $22 \pm 4$                                    | $120 \pm 28$                          |
|           | mechanism                    | noncompetitive                                | partial                               |
| <b>18</b> | $K_i$ ( $\mu\text{M}$ )      |   | $31 \pm 10$                           |
|           | $K_{is}$ ( $\mu\text{M}$ )   | $8.7 \pm 0.9$                                 | $36 \pm 12$                           |
|           | Mechanism                    | Noncompetitive                                | Partial                               |
| <b>19</b> | $K_i$ ( $\mu\text{M}$ )      | $6.7 \pm 1.6$                                 | $312 \pm 182$                         |
|           | $K_{is}$ ( $\mu\text{M}$ )   | $16 \pm 4$                                    | $57 \pm 12$                           |
|           | mechanism                    | partial                                       | partial                               |
| <b>21</b> | $K_i$ ( $\mu\text{M}$ )      | $16 \pm 8$                                    | $135 \pm 20$                          |
|           | $K_{is}$ ( $\mu\text{M}$ )   | $10 \pm 2$                                    |                                       |
|           | mechanism                    | partial                                       | competitive                           |
| <b>22</b> | $K_i$ ( $\mu\text{M}$ )      | $23 \pm 14$                                   | $61 \pm 13$                           |
|           | $K_{is}$ ( $\mu\text{M}$ )   | $10 \pm 2$                                    | $104 \pm 22$                          |
|           | mechanism                    | partial                                       | partial                               |

<sup>a</sup>  $K_i$  is the inhibitor dissociation constant for the process  $\text{E} + \text{I} \rightleftharpoons \text{EI}$ .  
<sup>b</sup>  $K_{is}$  is the inhibitor dissociation constant for the process  $\text{ES} + \text{I} \rightleftharpoons \text{ESI}$ .

Since the folding topologies and the amino acids of *E. coli* and *S. pombe* enzymes in direct contact with the bound ligands are closely similar, the structure of the *E. coli* active site with bound ligands can be proposed by combining elements of the two structures. The two ligand molecules of 6-carboxyethyl-7-oxo-8-ribityllumazine (**23**) in the N-terminal barrel (acceptor site) and C-terminal barrel (donor site) were removed from the enzyme structure, and two molecules of compound **15** were then docked sequentially in the two sites by using GOLD software (BST, version 3.0, 2005), which docks a flexible ligand into a semiflexible protein structure.<sup>38</sup> Energy minimization was performed by using Sybyl 8.0 and the MMFF94s force field. All possible docking patterns for different ligand configuration combinations (RR, SS, RS, SR in acceptor site and donor site, respectively) were analyzed and the RS combination had the highest binding energy (Supporting Information, Table S1). The structure of the RS combination having the highest GOLD score is displayed in Figure 2. The binding is stabilized

(38) Jones, G.; Willett, P.; Glen, R. C.; Leach, A. R.; Taylor, R. J. *Mol. Biol.* **1997**, 267, 727–748.

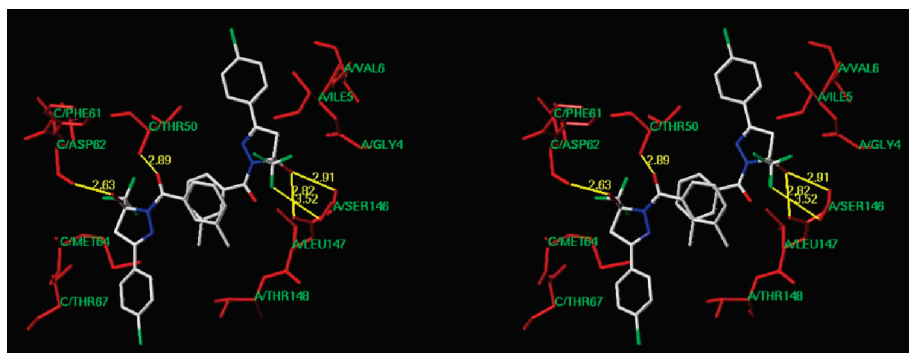
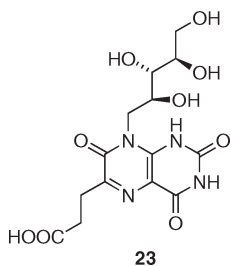


**FIGURE 2.** Hydrogen bonding network existing in the hypothetical active site binding model of *E. coli* riboflavin synthase with compound **15** (R in the acceptor site and S in the donor site). The amino acid residues are red and labeled by chain/residue names, and the ligands are colored by atom type. The diagram is programmed for wall-eyed (relaxed) viewing.

by stacking interactions between one benzene ring of each compound **15** in the binding pocket, with the remaining two benzene rings pointing in opposite directions, which is consistent with the stacking pattern of the substrate shown in Figure 1. In addition, the binding of compound **15** to the enzyme could be mediated by hydrogen bonding interactions involving the backbone nitrogen of Thr50 and the backbone oxygen of Asp62 from the acceptor site, as well as the backbone nitrogen, backbone oxygen, and side chain oxygen of Ser146 from the donor site.



Since all six compounds had been shown to inhibit *M. tuberculosis* riboflavin synthase, they were evaluated for their activity against the *M. tuberculosis* strain H<sub>37</sub>Rv (replicating phenotype, R-TB) by using MABA<sup>39,40</sup> (microplate alamar blue assay) and *M. tuberculosis* strain H<sub>37</sub>Rv-CA-luxAB (nonreplicating persistent phenotype, NRP-TB) by using LORA (low oxygen recovery assay) methods.<sup>41,42</sup> Among the compounds shown in Table 2, three riboflavin synthase inhibitors **16**, **18**, and **22** exhibited moderate antibiotic activity against replicating *M. tuberculosis* (MIC = 36.6, 36.5, and 50.5  $\mu$ M, respectively, vs. 0.08  $\mu$ M for rifampin and 0.47  $\mu$ M for isoniazid) and nonreplicating *M. tuberculosis* (MIC = 48.9, 63.7, and 56.0  $\mu$ M vs. 0.85  $\mu$ M for rifampin and >128  $\mu$ M for isoniazid).

In conclusion, a novel inhibitor of riboflavin synthase was discovered by high-throughput screening and its structure was corrected, and a series of its analogues with different

**TABLE 2.** In vitro Activity of Compounds 15-22 Against *M. tuberculosis*

| compd                      | MIC ( $\mu$ M) <sup>a</sup> |                   |
|----------------------------|-----------------------------|-------------------|
|                            | MABA <sup>b</sup>           | LORA <sup>c</sup> |
| <b>15</b>                  | > 128                       | > 128             |
| <b>16</b>                  | 36.6 $\pm$ 3.7              | 48.9 $\pm$ 0.9    |
| <b>18</b>                  | 36.5 $\pm$ 0.8              | 63.7 $\pm$ 3.4    |
| <b>19</b>                  | > 128                       | > 128             |
| <b>21</b>                  | > 128                       | > 128             |
| <b>22</b>                  | 50.5 $\pm$ 3.6              | 56.0 $\pm$ 3.5    |
| rifampin (RMP)             | 0.08                        | 0.85              |
| isoniazid (INH)            | 0.47                        | > 128             |
| nitroimidazopyran (PA 824) | 0.49                        | 1.31              |

<sup>a</sup> MIC = minimum inhibitory concentration. <sup>b</sup> MABA = microplate Alamar Blue assay. <sup>c</sup> LORA = low oxygen recovery assay (luciferase readout).

aromatic substituent positions were prepared and evaluated for inhibition of *M. tuberculosis* and *E. coli* riboflavin synthases. All of the compounds were evaluated for activity against both R-TB and NRP-TB *M. tuberculosis* phenotypes by making use of both the MABA and LORA methods. All six compounds showed moderate inhibition in enzyme kinetic studies and three of them exhibit activity against *M. tuberculosis*. This study provides possible leads for the design of new riboflavin synthase inhibitors as potential antitubercular agents. This is the first report of riboflavin synthase inhibitors with antibiotic activity. However, the evidence that inhibition of *M. tuberculosis* riboflavin synthase is responsible for the antibiotic activity is circumstantial at the present time, and off-target effects may contribute. On the basis of the structures of the pyrazoles reported in this study, other targets that should be considered include *M. tuberculosis* CYP51,<sup>43,44</sup> *M. tuberculosis* CYP121,<sup>43,44</sup> and *M. tuberculosis* UDP-galactopyranose mutase (UGM).<sup>45</sup> Structurally related pyrazoles that have antibiotic activity vs. *M. tuberculosis* have also recently been reported without target identification.<sup>46</sup>

(39) Collins, L. A.; Franzblau, S. G. *Antimicrob. Agents Chemother.* **1997**, *41*, 1004–1009.

(40) Falzari, K.; Zhu, Z. H.; Pan, D. H.; Liu, H. W.; Hongmancee, P.; Franzblau, S. G. *Antimicrob. Agents Chemother.* **2005**, *49*, 1447–1454.

(41) Jayaprakash, S.; Iso, Y.; Wan, B.; Franzblau, S. G.; Kozikowski, A. P. *ChemMedChem* **2006**, *1*, 593–.

(42) Bate, A. B.; Kalin, J. H.; Fooksman, E. M.; Amorose, E. L.; Price, C. M.; Williams, H. M.; Rodig, M. J.; Mitchell, M. O.; Cho, S. H.; Wang, Y. H.; Franzblau, S. G. *Bioorg. Med. Chem. Lett.* **2007**, *17*, 1346–1348.

(43) McLean, K. J.; Marshall, K. R.; Richmond, A.; Hunter, I. S.; Fowler, K.; Kieser, T.; Gurcha, S. S.; Besra, G. S.; Munro, A. W. *Microbiology (Reading, U.K.)* **2002**, *148*, 2937–2949.

(44) Menozzi, G.; Merello, L.; Fossa, P.; Schenone, S.; Ranise, A.; Mosti, L.; Bondavalli, F.; Loddo, R.; Murgioni, C.; Mascia, V.; La Colla, P.; Tamburini, E. *Bioorg. Med. Chem.* **2004**, *12*, 5465–5483.

(45) Carlson, E. E.; May, J. F.; Kiessling, L. L. *Chem. Biol.* **2006**, *13*, 825–837.

(46) Castagnolo, D.; De Logu, A.; Radi, M.; Bechi, B.; Manetti, F.; Magnani, M.; Supino, S.; Meleddu, R.; Chisu, L.; Botta, M. *Bioorg. Med. Chem.* **2008**, *16*, 8587–8591.

## Experimental Section

**<sup>19</sup>F NMR Spectroscopy.** The <sup>19</sup>F NMR chemical shifts are reported relative to CF<sub>3</sub>COOH (external standard).

**[3-(4-Chlorophenyl)-5-hydroxy-5-(trifluoromethyl)-4,5-dihydro-1H-pyrazol-1-yl](*m*-tolyl)methanone (15).** 1-(4-Chlorophenyl)-4,4,4-trifluoro-1,3-butanedione (751.8 mg, 3 mmol) was added to a stirred solution of *m*-toluic hydrazide (450.54 mg, 3 mmol) in ethanol (50 mL). The mixture was heated at reflux for 10 h. Concentrated HCl (2 mL) was added to the reaction mixture, which was then stirred for another 2 h. Removal of the solvent produced a yellow oil, which was subjected to silica gel column chromatography, eluting with dichloromethane–hexane 3:1, to afford white crystals (702.3 mg, 61.2%); mp 94–95 °C. The mixed mp of **15** and the commercial sample **CD 3852-0429** was 79–95 °C. IR (KBr) 3379, 1648 cm<sup>-1</sup>; <sup>1</sup>H NMR (300 MHz, CDCl<sub>3</sub>) δ 7.84–7.81 (m, 2 H), 7.57–7.54 (m, 2 H), 7.40–7.35 (m, 4 H), 6.87 (s, 1 H), 3.72 (d, *J* = 18.57 Hz, 1 H), 3.54 (d, *J* = 18.57 Hz, 1 H), 2.45 (s, 3 H); <sup>13</sup>C NMR (75 MHz, CDCl<sub>3</sub>) δ 171.2, 152.00, 137.6, 137.00, 133.0, 132.8, 130.7, 129.4, 128.4, 127.9, 127.7, 127.5, 123.4 (q, *J* = 285.2 Hz), 93.05 (q, *J* = 33.7 Hz), 42.9, 21.2; <sup>19</sup>F NMR (300 MHz, CDCl<sub>3</sub>) δ -3.11 (s, 3 F); negative ion ESIMS *m/z* 381 {[M(CI<sup>35</sup>) - H<sup>+</sup>]<sup>-</sup>, 100}, 383 {[M(CI<sup>37</sup>) - H<sup>+</sup>]<sup>-</sup>, 27}, negative ion HR ESIMS calcd for (M - H<sup>+</sup>)<sup>-</sup> 381.0618, found 381.0624. The crystal structure was solved by X-ray diffraction analysis and the data are summarized as follows: C<sub>18</sub>H<sub>14</sub>ClF<sub>3</sub>N<sub>2</sub>O<sub>2</sub>; FW = 382.77; *a* = 15.9749(2) Å; *b* = 16.4925(3) Å; *c* = 27.4117(6) Å; α = 81.5285 (7)°; β = 82.2566(7)°; γ = 89.0766(14)°; vol = 7078.1(2) Å<sup>3</sup>; triclinic; space group *P*1̄ (No. 2); *Z* = 16; crystal size = 0.35 × 0.28 × 0.13 mm<sup>3</sup>; GOF = 1.111; *R*(*F*<sub>o</sub>) = 0.075; *R*<sub>w</sub>(*F*<sub>o</sub><sup>2</sup>) = 0.123. Anal. Calcd for C<sub>18</sub>H<sub>14</sub>ClF<sub>3</sub>N<sub>2</sub>O<sub>2</sub>: C, 56.48; H, 3.69; N, 7.32. Found: C, 56.33; H, 3.66; N, 7.22.

**[5-(4-Chlorophenyl)-5-hydroxy-3-(trifluoromethyl)-4,5-dihydro-1H-pyrazol-1-yl](*m*-tolyl)methanone (16).** Compound **16** was separated from **15** by silica gel column chromatography, eluting with dichloromethane–hexane 3:1, to afford a light yellow powder (72.4 mg, 6.3%); mp 172–173 °C. IR (KBr) 3391, 1652 cm<sup>-1</sup>; <sup>1</sup>H NMR (300 MHz, CDCl<sub>3</sub>) δ 7.72–7.69 (m, 2 H), 7.43–7.32 (m, 6 H), 5.22 (s, 1 H), 3.49 (d, *J* = 19.14 Hz, 1 H), 3.17 (d, *J* = 19.14 Hz, 1 H), 2.39 (s, 3 H); <sup>13</sup>C NMR (75 MHz, CDCl<sub>3</sub>) δ 169.4, 143.6 (q, *J* = 38.72 Hz), 140.6, 137.9, 134.6, 133.4, 131.9, 130.7, 129.2, 127.9, 127.4, 125.5, 119.53 (q, *J* = 269.4 Hz), 95.6, 47.4, 21.3; <sup>19</sup>F NMR (300 MHz, CDCl<sub>3</sub>) δ 10.33 (s, 3 F); ESIMS *m/z* 405 [M(CI<sup>35</sup>)Na<sup>+</sup>, 100], 407 [M(CI<sup>37</sup>)Na<sup>+</sup>, 33], negative ion ESIMS 381 {[M(CI<sup>35</sup>) - H<sup>+</sup>]<sup>-</sup>, 100}, 383 {[M(CI<sup>37</sup>) - H<sup>+</sup>]<sup>-</sup>, 25}, HR ESIMS calcd for [M(CI<sup>35</sup>)Na<sup>+</sup>] 405.0594, found 405.0601.

**[3-(4-Chlorophenyl)-5-hydroxy-5-(trifluoromethyl)-4,5-dihydro-1H-pyrazol-1-yl](*o*-tolyl)methanone (18).** 1-(4-Chlorophenyl)-4,4,4-trifluoro-1,3-butanedione (250.6 mg, 1 mmol) was added to a stirred solution of *o*-toluic hydrazide (150.2 mg, 1 mmol) in ethanol (17 mL). The mixture was heated at reflux for 10 h. Removal of the solvent produced a yellow oil, which was subjected to silica gel column chromatography, eluting with dichloromethane–hexane 3:1, to afford a white powder (147.7 mg, 38.7%); mp 77–78 °C. The mixed mp of **18** and the commercial sample **CD 3852-0429** was 79–81 °C. IR (KBr) 3392, 1652 cm<sup>-1</sup>; <sup>1</sup>H NMR (300 MHz, CDCl<sub>3</sub>) δ 7.49–7.26 (m, 8 H), 6.59 (s, 1 H), 3.72 (d, *J* = 18.57 Hz, 1 H), 3.57 (d, *J* = 18.62 Hz, 1 H), 2.41 (s, 3 H); <sup>13</sup>C NMR (125 MHz, CDCl<sub>3</sub>) δ 172.4, 152.4, 137.2, 136.2, 134.2, 130.47, 130.4, 129.1, 128.3, 128.2, 127.9, 125.3, 123.4 (q, *J* = 285.88 Hz), 92.4 (q, *J* = 34.04 Hz), 43.3, 19.6; <sup>19</sup>F NMR (300 MHz, CDCl<sub>3</sub>) δ -3.55 (s, 3 F); ESIMS *m/z* 381 {[M(CI<sup>35</sup>)H<sup>+</sup>]<sup>+</sup>, 100}, 383 {[M(CI<sup>37</sup>)H<sup>+</sup>]<sup>+</sup>, 33}, negative ion HR ESIMS calcd for (M - H<sup>+</sup>)<sup>-</sup> 381.0618, found 381.0610. Anal. Calcd for C<sub>18</sub>H<sub>14</sub>ClF<sub>3</sub>N<sub>2</sub>O<sub>2</sub>: C, 56.48; H, 3.69; N, 7.32. Found: C, 56.40; H, 3.67; N, 7.27.

**[5-(4-Chlorophenyl)-5-hydroxy-3-(trifluoromethyl)-4,5-dihydro-1H-pyrazol-1-yl](*o*-tolyl)methanone (19).** Compound **19** was separated from **18** by silica gel column chromatography, eluting with dichloromethane–hexane 3:1, to afford a light yellow powder (28.6 mg, 7.5%); mp 201–202 °C. IR (KBr) 3401, 1666 cm<sup>-1</sup>; <sup>1</sup>H NMR (300 MHz, CDCl<sub>3</sub>) δ 7.46–7.36 (m, 6 H), 7.28–7.23 (m, 2 H), 5.29 (s, 1 H), 3.55 (d, *J* = 18.57 Hz, 1 H), 3.21 (d, *J* = 19.45 Hz, 1 H), 2.37 (s, 3 H); <sup>13</sup>C NMR (75 MHz, CDCl<sub>3</sub>) δ 171.0, 143.9 (q, *J* = 38.9 Hz), 140.7, 136.5, 134.8, 133.0, 130.7, 129.2, 128.4, 125.4, 125.3, 121.2, 119.4 (q, *J* = 269.7 Hz), 94.9, 48.00, 19.8; <sup>19</sup>F NMR (300 MHz, CDCl<sub>3</sub>) δ 10.28 (s, 3 F); negative ion ESIMS *m/z* 381 {[M(CI<sup>35</sup>) - H<sup>+</sup>]<sup>-</sup>, 100}, 383 {[M(CI<sup>37</sup>) - H<sup>+</sup>]<sup>-</sup>, 29}, negative ion HR ESIMS calcd for (M - H<sup>+</sup>)<sup>-</sup> 381.0618, found 381.0618.

**[3-(4-Chlorophenyl)-5-hydroxy-5-(trifluoromethyl)-4,5-dihydro-1H-pyrazol-1-yl](*p*-tolyl)methanone (21).** 1-(4-Chlorophenyl)-4,4,4-trifluoro-1,3-butanedione (250.6 mg, 1 mmol) was added to a stirred solution of *p*-toluic hydrazide (150.2 mg, 1 mmol) in ethanol (17 mL). The mixture was heated under reflux for 10 h. Removal of the solvent produced a yellow oil, which was subjected to silica gel chromatography with mobile phase dichloromethane–hexane 3:1 to afford **21** as white crystals (61.5 mg, 16.1%); mp 125–126 °C. IR (KBr) 3369, 1647 cm<sup>-1</sup>; <sup>1</sup>H NMR (300 MHz, CDCl<sub>3</sub>) δ 7.90 (d, *J* = 8.20 Hz, 2 H), 7.57 (dt, *J*<sub>1</sub> = 8.58 Hz, *J*<sub>2</sub> = 1.87 Hz, 2 H), 7.40 (dt, *J*<sub>1</sub> = 8.52 Hz, *J*<sub>2</sub> = 1.76 Hz, 2 H), 7.29 (d, *J* = 8.02 Hz, 2 H), 6.80 (s, 1 H), 3.70 (d, *J* = 18.55 Hz, 1 H), 3.53 (d, *J* = 18.58 Hz, 1 H), 2.45 (s, 3 H); <sup>13</sup>C NMR (75 MHz, CDCl<sub>3</sub>) δ 171.1, 151.8, 143.1, 137.1, 130.5, 129.8, 129.1, 128.6, 128.4, 127.9, 123.4 (q, *J* = 285.45 Hz), 93.1 (q, *J* = 33.9 Hz), 43.00, 21.6; <sup>19</sup>F NMR (300 MHz, CDCl<sub>3</sub>) δ -3.35 (s, 3 F); ESIMS *m/z* 405 (M(CI<sup>35</sup>)Na<sup>+</sup>, 100), 407 (M(CI<sup>37</sup>)Na<sup>+</sup>, 30); negative ion ESIMS 381 {[M(CI<sup>35</sup>) - H<sup>+</sup>]<sup>-</sup>, 100}, 383 {[M(CI<sup>37</sup>) - H<sup>+</sup>]<sup>-</sup>, 27}, negative ion HR ESIMS calcd for (M - H<sup>+</sup>)<sup>-</sup> 381.0618, found 381.0620. Anal. Calcd for C<sub>18</sub>H<sub>14</sub>ClF<sub>3</sub>N<sub>2</sub>O<sub>2</sub>: C, 56.48; H, 3.69; N, 7.32. Found: C, 56.42; H, 3.65; N, 7.21.

**[5-(4-Chlorophenyl)-5-hydroxy-3-(trifluoromethyl)-4,5-dihydro-1H-pyrazol-1-yl](*p*-tolyl)methanone (22).** Compound **22** was separated from **21** by silica gel column chromatography, eluting with dichloromethane–hexane 3:1, to afford yellow crystals (10 mg, 2.6%); mp 159–160 °C. IR (KBr) 3436, 1655 cm<sup>-1</sup>; <sup>1</sup>H NMR (300 MHz, CDCl<sub>3</sub>) δ 7.85 (d, *J* = 8.22 Hz, 2 H), 7.41 (dq, *J*<sub>1</sub> = 8.72 Hz, *J*<sub>2</sub> = 2.20 Hz, 4 H), 7.27 (t, *J*<sub>1</sub> = *J*<sub>2</sub> = 4.54 Hz, 2 H), 5.22 (s, 1 H), 3.50 (d, *J* = 19.05 Hz, 1 H), 3.19 (d, *J* = 19.13 Hz, 1 H), 2.43 (s, 3 H); <sup>13</sup>C NMR (75 MHz, CDCl<sub>3</sub>) δ 169.1, 143.4, 143.4 (q, *J* = 38.93 Hz), 140.6, 134.6, 130.4, 129.3, 129.1, 128.9, 128.72, 125.46, 119.49 (q, *J* = 269.65 Hz), 95.6, 47.2, 21.6; <sup>19</sup>F NMR (300 MHz, CDCl<sub>3</sub>) δ 10.32 (s, 3 F); ESIMS *m/z* 405 [M(CI<sup>35</sup>)Na<sup>+</sup>, 100], 407 [M(CI<sup>37</sup>)Na<sup>+</sup>, 32], negative ion ESIMS 381 {[M(CI<sup>35</sup>) - H<sup>+</sup>]<sup>-</sup>, 100}, 383 {[M(CI<sup>37</sup>) - H<sup>+</sup>]<sup>-</sup>, 26}, HR ESIMS calcd for (MNa<sup>+</sup>) 405.0594, found 405.0602.

**Acknowledgment.** This research was made possible by NIH grant GM51469, the Fonds der Chemischen Industrie, and the Hans Fischer Gesellschaft. Some of this research was conducted in a facility constructed with the financial support of a Research facilities Improvement program grant C06-14499 from the National Institutes of Health.

**Supporting Information Available:** Figures of hypothetical *E. coli* riboflavin synthase active site models with other configurations of compound **15**, the NMR spectra of all compounds, the CIF file for the crystal structure of dihydropyrazole **15**, the molecular modeling procedure for compound **15** (Figure 2), the riboflavin synthase inhibition assay procedure, and the *M. tuberculosis* inhibition assay procedure. This material is available free of charge via the Internet at <http://pubs.acs.org>.